Supplementary Information

for

A Power-Efficient Coplanar Waveguide Design for Enhanced Optical Readout in hBN Quantum Sensors

Songtao Wu[1†], Biswajit Sahoo[1,5†], Naveed Hussain[1†], Alejandro Ruiz[1], Sumukh Vaidya[3], Saakshi Dikshit[4], Hayate Yamano[2], Katsunori Danno[2], Chen Ling[1], Shougo Higashi[1,2], Tongcang Li[3,4], Debasish Banerjee[1]*

Address 1: Toyota Research Institute of North America, Ann Arbor, MI, USA 48105

*Email: Debasish.banerjee@toyota.com

Address 2: Material Engineering Division, Toyota Motor Corporation, Aichi, Japan, 471-8572

*Email: Shougo.higashi@toyota.com

Address 3: Department of Physics and Astronomy, Purdue University, West Lafayette, Indiana 47907, United States

Address 4: Elmore Family School of Electrical and Computer Engineering, Purdue University, West Lafayette, Indiana, 47907, United States

Address 5: Department of Physics, University of California, San Diego, CA 92093, USA

† These authors contributed equally to this work

Methods

Quantum Sensing Device Fabrication

The results from our simulations informed the fabrication process for Gen 2 and 3 devices. Gen 2 and 3 devices were fabricated on Si/SiO_2, Si/SiO_2, and C-Plane (0001) sapphire substrates, respectively. This intricate procedure relies on a single-step lift-off technique enabled by ultraviolet (UV) photolithography. To ensure proper adhesion for the subsequent layer, a thin film of titanium (Ti), typically around 10 nanometers (nm) thick, is deposited first. This initial layer acts like a bridge, allowing for a thicker layer of gold (Au), typically around 200 nm thick, to be deposited on top. Together, these combined metal layers (Ti/Au) form the coplanar waveguide (CPW) structures. These waveguides will serve as the guiding pathways for the crucial MW signals within the device.

V_B^- *Defect implantation*

The next step involves the creation of spin-active V_B^--rich h-BN flakes that are mechanically exfoliated on Si/SiO_2 substrate. The hBN flakes are mechanically exfoliated onto a Si/SiO_2 substrate. Helium ions (He^+) with a precisely controlled dose rate (*~*10^{13}*-*10^{14} *ions/cm²)* and a specific irradiation duration (*300-400 seconds*) have been used to deterministically create boron vacancies (V_B^-). Optimizing these parameters is crucial, as they dictate the density and depth of V_B^- defects created within the h-BN flakes.

Transfer of hBN flake onto the Waveguide:

After ion implantation, hBN flakes were transferred onto gold waveguide of all devices. A stamp, composed of a polycarbonate (PC) film on a polydimethylsiloxane (PDMS) block, was utilized to pick up and transfer the hBN flakes. The stamp was positioned on a glass slide attached to a micromanipulator under a microscope (2D Heterostructure Transfer System, hq graphene). The Si substrate, containing the hBN flakes, was secured on a heated stage. The PC stamp was brought into contact with selected flakes. The stage was heated to 145°C and cooled gradually. The PC stamp was lifted at 60°C. The Si substrate was removed, and the target substrate was placed on the heated stage. The flakes were positioned over the constricted region of the plasmonic waveguide. The PC stamp and target substrate were brought into contact. The stage was heated to 165°C and cooled gradually. The glass slide with the PDMS block was lifted. The PC stamp remained on the target substrate. Chloroform was used to dissolve the PC stamp and clean the substrate surface.

Confocal Microscopy:

Optical measurements were conducted at room temperature under ambient conditions using a custom-built confocal microscope system. A 532-nm laser was directed through a 550-nm dichroic mirror and focused onto the sample using a high numerical aperture (NA=0.9) objective lens with 100X magnification. An acousto-optic modulator (ISOMET, M1205-T110L-1) served as a rapid optical switch. The PL was separated from the laser by a dichroic mirror, and any residual laser light was absorbed by two 550-nm long-pass filters and a 700nm longpass filter. Subsequently, the PL was coupled into a 125-um single-mode fiber and directed to either a single-photon counter (Excelitas, SPCM-AQRH) or a spectrometer (Andor shamrock SR-500).

ODMR Measurements

Continuous wave ($C.W.$) ODMR measurements were conducted using a custom-built confocal microscope system. A 532-nm laser was directed through a 550-nm dichroic mirror and focused onto the sample using a high numerical aperture (NA = 0.9) objective lens with ×100 magnification. An acousto-optic modulator (ISOMET, M1205-T110L-1) served as a rapid optical switch. The PL was separated from the laser by the dichroic mirror, and any residual laser light was blocked by two 550-nm long-pass filters and a 700 nm long pass filter. Subsequently, the PL was coupled into an optical fiber and directed to a single-photon counter (Excelitas, SPCM-AQRH). The MW signal was generated by a Stanford Research Systems SG386 signal generator. The amplitude was modulated by two fast RF switches (Mini-Circuits ZASWA-2-50DRA+) and then amplified by an amplifier (Mini-circuits ZHL-10W-202s or ZHL-16W-43-s+). For ODMR measurements, a pulse streamer (Swabian Instruments Pulse Streamer 8/2) sent pulses to modulate the RF switches, signal generator, and AOM. A permanent magnet mounted on a translation stage combined with a goniometer behind the sample enabled the application of a tunable external DC magnetic field.

Simulation and Device Scaling:

Figure S2 (a)-(c) shows the r.f. magnetic field accumulation as obtained by COMSOL simulation at the active area for the working range of frequencies.

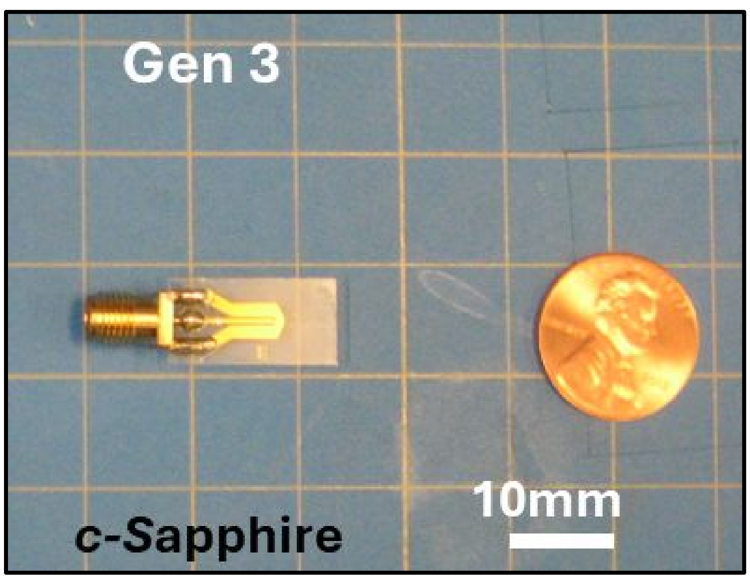

Fig. S1. Optical micrograph showing the scalability of the waveguide design (Gen 2) onto a 10×10 mm^2 Si/SiO$_2$ substrate.

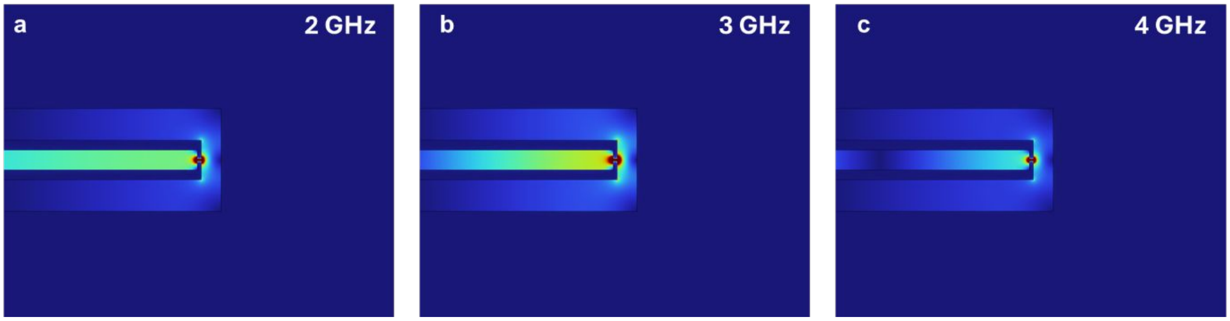

Fig. S2. **(a-c)** Field accumulation at various MW frequencies as obtained by simulation performed on COMSOL Multiphysics.

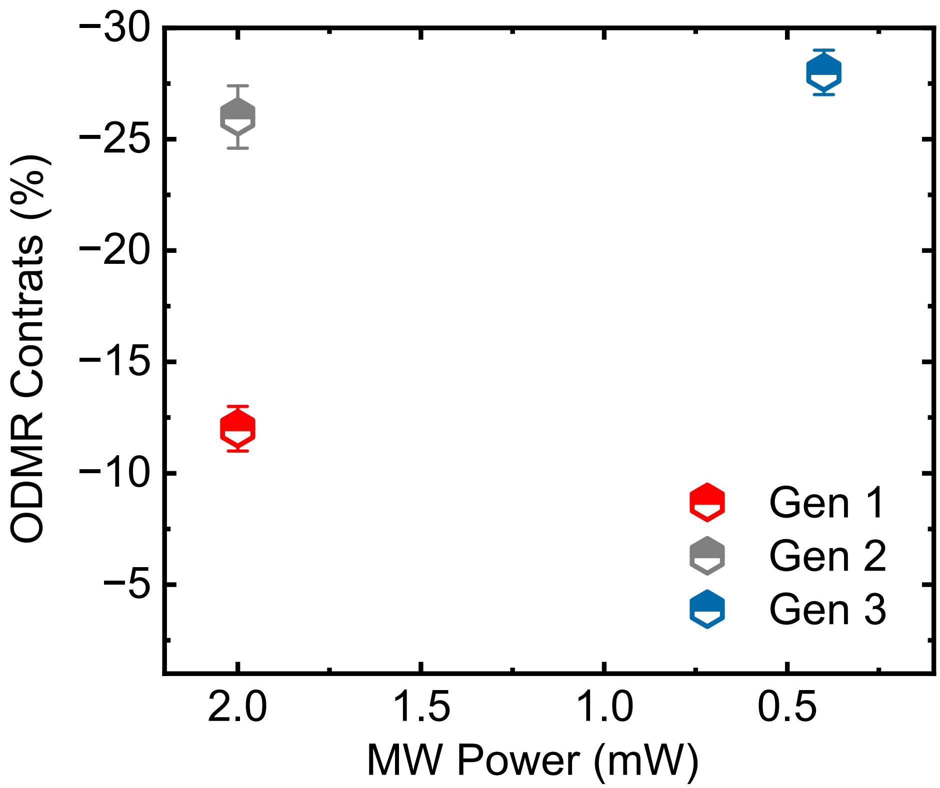

Fig. S3. The ODMR contrast for each generation, measured at its corresponding microwave power.

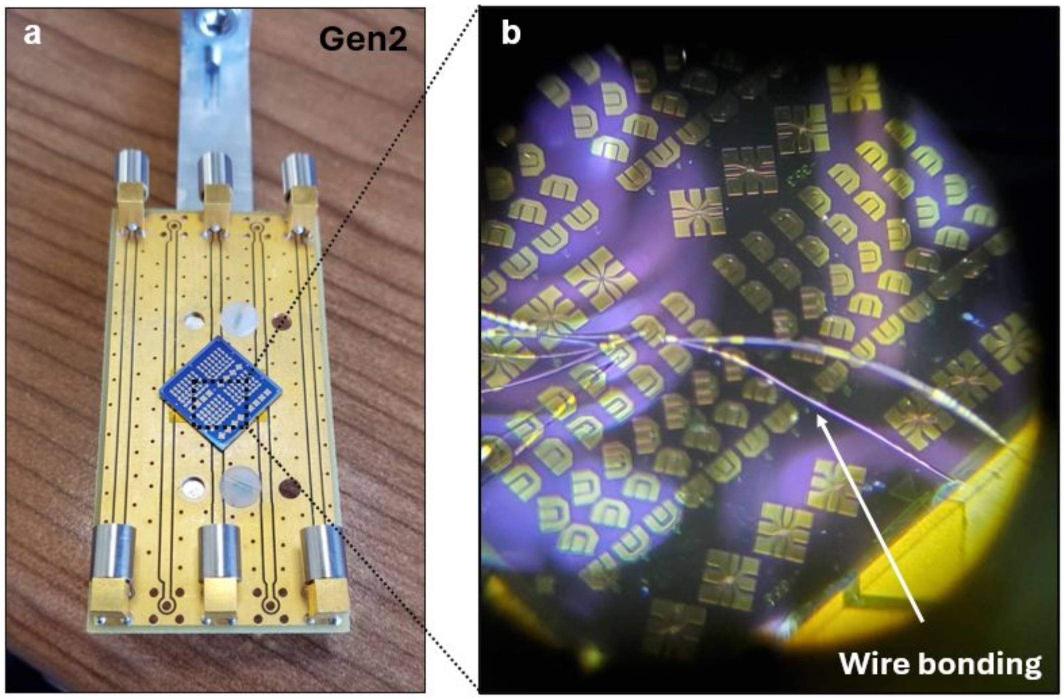

Fig. S4. **(a)** Optical micrograph showing the scalability of the waveguide design (Gen 2) onto a 10×10 mm^2 Si/SiO_2 substrate. **(b)** A zoomed-in optical image showing wire-bonded connections.

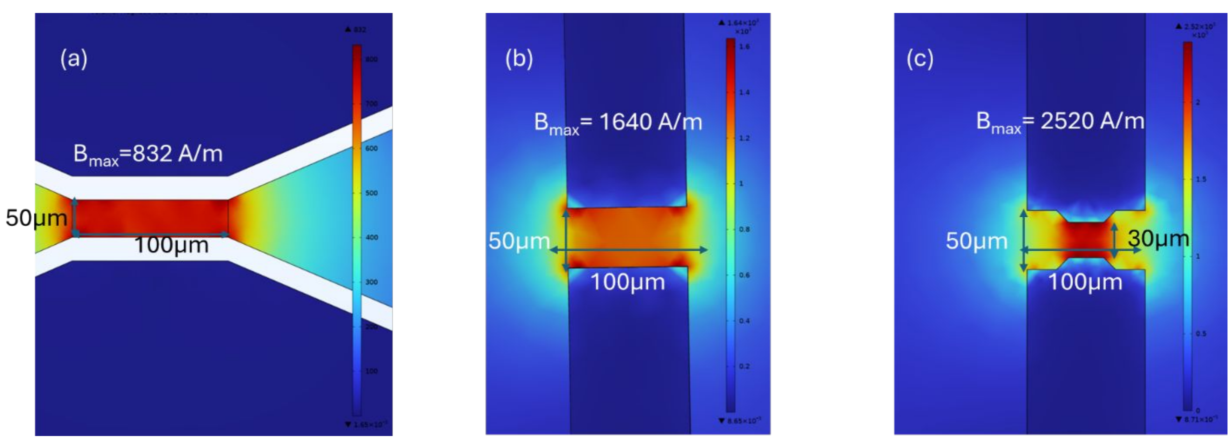

Figure S5 (a)-(c) show the COMSOL simulations of the open and shorted waveguides for the same antenna length demonstrating enhanced magnetic field concentration in the shorted devices.

Table 1: Values of *I, C,* and *Δv* for the different generations

Parameter	**Symbol (Unit)**	**Gen 1**	**Gen 2**	**Gen 3**
Photoluminescence (PL)	I (cnts. /sec)	14000	25000	59000
ODMR Contrast	C (%)	12	26	28
Linewidth	Δv (MHz)	190	176	180
DC Field Sensitivity	η_{DC} ($\mu T/\sqrt{Hz}$)	368	117.7	72.7